

## PBT-6, a Novel PI3KC2 $\gamma$ Inhibitor in Rheumatoid Arthritis

Juyoung Kim<sup>1,†</sup>, Kyung Hee Jung<sup>1,†</sup>, Jaeho Yoo<sup>2,†</sup>, Jung Hee Park<sup>1</sup>, Hong Hua Yan<sup>1</sup>, Zhenghuan Fang<sup>1</sup>, Joo Han Lim<sup>1</sup>, Seong-Ryul Kwon<sup>1</sup>, Myung Ku Kim<sup>1</sup>, Hyun-Ju Park<sup>2</sup> and Soon-Sun Hong<sup>1,\*</sup>

<sup>1</sup>Department of Medicine, College of Medicine, Inha University, Incheon 22313,

<sup>2</sup>School of Pharmacy, Sungkyunkwan University, Suwon 16419, Republic of Korea

### Abstract

Phosphoinositide 3-kinase (PI3K) is considered as a promising therapeutic target for rheumatoid arthritis (RA) because of its involvement in inflammatory processes. However, limited studies have reported the involvement of PI3KC2 $\gamma$  in RA, and the underlying mechanism remains largely unknown. Therefore, we investigated the role of PI3KC2 $\gamma$  as a novel therapeutic target for RA and the effect of its selective inhibitor, PBT-6. In this study, we observed that PI3KC2 $\gamma$  was markedly increased in the synovial fluid and tissue as well as the PBMCs of patients with RA. PBT-6, a novel PI3KC2 $\gamma$  inhibitor, decreased the cell growth of TNF-mediated synovial fibroblasts and LPS-mediated macrophages. Furthermore, PBT-6 inhibited the PI3KC2 $\gamma$  expression and PI3K/AKT signaling pathway in both synovial fibroblasts and macrophages. In addition, PBT-6 suppressed macrophage migration via CCL2 and osteoclastogenesis. In CIA mice, it significantly inhibited the progression and development of RA by decreasing arthritis scores and paw swelling. Three-dimensional micro-computed tomography confirmed that PBT-6 enhanced the joint structures in CIA mice. Taken together, our findings suggest that PI3KC2 $\gamma$  is a therapeutic target for RA, and PBT-6 could be developed as a novel PI3KC2 $\gamma$  inhibitor to target inflammatory diseases including RA.

**Key Words:** Rheumatoid arthritis, Collagen-induced arthritis, PI3KC2 $\gamma$ , RANKL

### INTRODUCTION

Rheumatoid arthritis (RA) is a chronic autoimmune inflammatory disorder with a prevalence of about 1% in the general population. RA is characterized by chronic inflammation in joints associated with synovial hyperplasia and infiltration of inflammatory cells into the synovial tissue. RA consequently causes joint stiffness and the progressive destruction of the articular cartilage and bone, placing a heavy burden on the individual and the society (Pap and Korb-Pap, 2015). RA is presented with multiple manifestations of inflammation due to complex causes; thus, various immune cells are involved in the development of inflammation (McInnes and Schett, 2011). In particular, the increase in macrophages in the synovium is an early hallmark of active rheumatic disease, and high numbers of macrophages are a prominent feature of inflammatory lesions (Udalova *et al.*, 2016). The activation of these cells can lead to the production of cytokines and mediators responsible for inflammation. Recently, abatacept, tocilizumab, rituximab, anakinra, infliximab, and etanercept have been used for treat-

ing RA (Frisell *et al.*, 2018). However, about 40% of RA patients do not respond to these therapeutics (Gillespie *et al.*, 2012). Considering the limited efficacy and adverse effects of current therapies, there is a critical need for novel targets and therapeutics for RA treatment.

Phosphoinositide 3-kinase (PI3K)/Akt signaling is a major regulator of inflammatory processes; thus, it has been considered as a promising drug target for the treatment of inflammatory and autoimmune diseases (Camps *et al.*, 2005). PI3Ks are lipid kinases that phosphorylate phosphoinositides at the 3'-OH position of the inositol ring, giving rise to PtdIns(3)P, PtdIns(3,4)P<sub>2</sub>, and PtdIns-(3,4,5)P<sub>3</sub> (Divecha and Irvine, 1995). PI3Ks have eight different isoforms in mammals, which are divided into three classes (class I, II, and III) depending on their sequence homology and substrate specificity (Vanhaesebroeck *et al.*, 1997). Of these, class I PI3Ks have been the most commonly investigated. Class I PI3Ks phosphorylate PI 4,5-diphosphate to produce PI 3,4,5-triphosphate and can be further subdivided into class IA (PI3K1 $\alpha$ , PI3K1 $\beta$ , and PI3K1 $\delta$  isoforms) and class IB (PI3K1 $\gamma$  isoform, class I

**Open Access** <https://doi.org/10.4062/biomolther.2019.153>

This is an Open Access article distributed under the terms of the Creative Commons Attribution Non-Commercial License (<http://creativecommons.org/licenses/by-nc/4.0/>) which permits unrestricted non-commercial use, distribution, and reproduction in any medium, provided the original work is properly cited.

Received Sep 18, 2019 Revised Oct 15, 2019 Accepted Oct 17, 2019

Published Online Nov 18, 2019

**\*Corresponding Author**

E-mail: hongss@inha.ac.kr

Tel: +82-32-890-3683, Fax: +82-32-890-2462

<sup>†</sup>The first three authors contributed equally to this work.

PI3K $\gamma$ ) (Pirola *et al.*, 2001). Among these isoforms, PI3KC1 $\delta$  and PI3KC1 $\gamma$  are emerging as novel therapeutic targets for treating inflammatory diseases (Rommel *et al.*, 2007; Harris *et al.*, 2009). Especially, PI3KC1 $\gamma$  is mainly expressed in hematopoietic cells, playing a critical role in chemokine signaling and the recruitment of immune cells including macrophages, neutrophils, and T cells (Li *et al.*, 2000). The defective migration of macrophages to injured sites and reduced chemoattractant-induced neutrophil respiratory burst have been observed in PI3KC1 $\gamma$  knockout mice (Hirsch *et al.*, 2000; Del Prete *et al.*, 2004). Considering the role of PI3KC1 $\gamma$  in inflammation, it is a potential therapeutic target for various inflammatory diseases in RA (Kim *et al.*, 2012; Boyle *et al.*, 2014). Indeed, the blockade of PI3KC1 $\gamma$  in CIA mouse models has been reported to suppress inflammatory damage in RA mice. In addition, a PI3K $\gamma$  inhibitor was found to reduce the clinical severity of arthritis and neutrophil accumulation in RA mouse models (Camps *et al.*, 2005). Thus far, the role and function of PI3KC1 $\gamma$  (class I PI3K) in various inflammatory diseases including RA have been extensively studied; however, little is known about the involvement of PI3KC2 $\gamma$  (class II PI3K $\gamma$ ) in inflammation and RA even though it has attracted attention as a potential drug target (Freitag *et al.*, 2015).

In this study, we investigated the association between PI3KC2 $\gamma$  and RA by evaluating the expression of PI3KC2 $\gamma$  in the serum and synovium of patients with RA. To target PI3KC2 $\gamma$ , we developed a novel oral PI3KC2 $\gamma$  inhibitor, PBT-6 (chemical name: 6-(4-pyridinyl)-2-benzothiazolamine), and the potential therapeutic targets of PBT-6 were validated in collagen-induced arthritis (CIA) mice. Furthermore, the underlying anti-arthritis mechanism of PBT-6 was investigated in synovial fibroblasts and macrophages.

## MATERIALS AND METHODS

### Chemicals and antibodies

Primary antibodies against PI3KC2 $\gamma$  (Thermo Fisher Scientific, Rockford, IL, USA), p-AKT1, p-AKT2, p-mTOR,  $\beta$ -actin (Cell Signaling Technology, Danvers, MA, USA), RANKL (Abcam, Cambridge, MA, UK), and NFATc1 (Santa Cruz Biotechnology, Dallas, CA, USA) were purchased. RANKL and M-CSF were obtained from R&D Systems (Minneapolis, MN, USA). In addition, method of PBT-6 synthesis was in detail described in supplementary method. In brief, the first step was the acetylation of NH<sub>2</sub> under mild conditions with pyridine and acetic anhydride. In the second step, bromo benzothiazol and boronic acid were coupled via the Suzuki reaction using a phosphine ligand, base, and Pd catalyst. In the final step, it was hydrolyzed in NaOH solution. 6-(pyridin-4-yl) benzo[d]thiazol-2-amine: <sup>1</sup>H NMR (400 MHz, DMSO): 8.58 (d, J=6, 2H-Ar), 8.18 (d, J=1.6, 1H-Ar), 7.70-7.66 (m, 5H), 7.42 (d, J=8, 1H-Ar).

### Kinase profiling

The activity of PBT-6, at a concentration of 1  $\mu$ M with an ATP concentration of 10  $\mu$ M, was screened against PI3 kinases by Eurofins (<https://www.eurofinsdiscoveryservices.com/>) using the Eurofins Kinase Profiler Selectivity Testing Service.

### PI3KC2 $\gamma$ kinase assay

The ADP-Glo Kinase Assay kit was obtained from Promega

(Madison, WI, USA). In a 1.5 mL microcentrifuge tube, 25  $\mu$ M of APT, 0.1 mg/mL of PI3K substrate, and various concentrations of PBT-6 (0.1-100  $\mu$ M) were added and followed by 5 ng/ $\mu$ L of PI3KC2 $\gamma$  enzyme. After incubation for 40 min at 30°C, 10  $\mu$ L of ADP-Glo™ reagent was added. After incubation for 40 min at 30°C, 10  $\mu$ L of kinase detection reagent was added and spun down. Finally, after transfer to a white plate, the luminescence was read.

### Cell culture

MH7A cells were purchased from Riken Cell Bank (Tsukuba, Japan) and cultured in RPMI1640 medium supplemented with 10% heat-inactivated fetal bovine serum (FBS) and 1% penicillin/streptomycin. Raw 264.7 cells were purchased from the Korean Cell Line Bank and cultured in Dulbecco's modified Eagle's medium (DMEM) supplemented with 10% heat-inactivated FBS and 1% penicillin/streptomycin. FBS and all other reagents used for cell culture were purchased from Invitrogen (Carlsbad, CA, USA). The cultures were maintained at 37°C in an incubator with a controlled humidified atmosphere composed of 95% air and 5% CO<sub>2</sub>.

### Measurement of cell viability

Cell viability was determined by MTT assay. In brief, the cells were seeded at a density of 8×10<sup>3</sup> cells/well in 96-well plates followed by overnight incubation. On the following day, the medium was removed, and the cells were treated with an inducer [TNF- $\alpha$  (50 ng/mL) or LPS (1  $\mu$ g/mL)] and various concentrations of PBT-6 (0.1-100  $\mu$ M). After incubation for 72 h, 10% of MTT solution (2 mg/mL) was added to each well, and the cells were incubated for another 4 h at 37°C. The formazan crystals obtained were dissolved in DMSO (100  $\mu$ L/well) with constant shaking for 5 min. The absorbance of the plate was then read with a microplate reader at 540 nm. Three replicate wells were evaluated for each analysis.

### Western blotting

The cells were washed with DPBS before they were lysed in lysis buffer containing protease and phosphatase inhibitors. Equal amounts of proteins were separated by 8, 12% sodium dodecyl sulfate-polyacrylamide gel electrophoresis and transferred to polyvinylidene fluoride membranes. Protein transfer was confirmed using Ponceau S staining solution (Sigma-Aldrich, St. Louis, MO, USA). The blots were then immunostained with the appropriate primary antibodies (1:1000) followed by secondary antibodies (1:5000) conjugated to horseradish peroxidase. The primary antibodies specific to the target proteins were detected manually using an X-Ray film by enhanced chemiluminescence (Amersham Biosciences, Piscataway, NJ, UK).

### Enzyme-linked immunosorbent assay (ELISA)

Informed consent was obtained from all of the patients, and the experimental protocol was approved by the Inha University Hospital Human Research Ethics Committee (INHAUH IRB 2015-09-016-002). In addition, we confirm that all experiments were performed in accordance with relevant guidelines and regulations. Peripheral blood and synovial fluid were collected from healthy control volunteers (HC, n=8), osteoarthritis patients (OA, n=9), and RA patients (RA, n=9). ELISA kits were purchased from R&D Systems, and cytokine levels in the serum or synovial fluid were measured according to the

manufacturer's instructions. In brief, each well was coated with 0.1 g of TNF- $\alpha$ , IL-1 $\beta$ , and IL-6 for 24 h and blocked with PBS containing 2% BSA for 1 h at room temperature. Then, serum or synovial fluid was added to each well and incubated for 24 h at 4°C. After washing the plate with PBS containing 0.1% Tween 20, biotinylated antibody was added to each well and reacted with streptavidin- horseradish peroxidase. After washing the plate, 3,3',5,5'-tetramethylbenzidine solution was added for 20 min. The reaction was stopped by the addition of 1 N sulfuric acid, and the signal was read at 450 nm. For *in vitro* cytokine secretion assay, MH7A cells ( $5 \times 10^4$ ) or Raw

264.7 cells ( $5 \times 10^6$ ) were seeded in 12-well plates and incubated with 1 and 10  $\mu$ M of PBT-6 for 6 h. Then, LPS or TNF- $\alpha$  was added for 24 h. The culture medium was harvested and used for cytokine measurements.

**PI3KC2 $\gamma$  siRNA transfection**

PI3KC2 $\gamma$  siRNA or negative control siRNA was purchased from Signal Chem (Richmond, BC, Canada). Cells ( $5 \times 10^5$  cells for MH7A and Raw 294.7) were transfected with 100 pM/ each well of either the PI3KC2 $\gamma$  siRNA or control siRNA using Lipofectamine 2000 (5  $\mu$ L/well, Invitrogen) in Opti-MEM

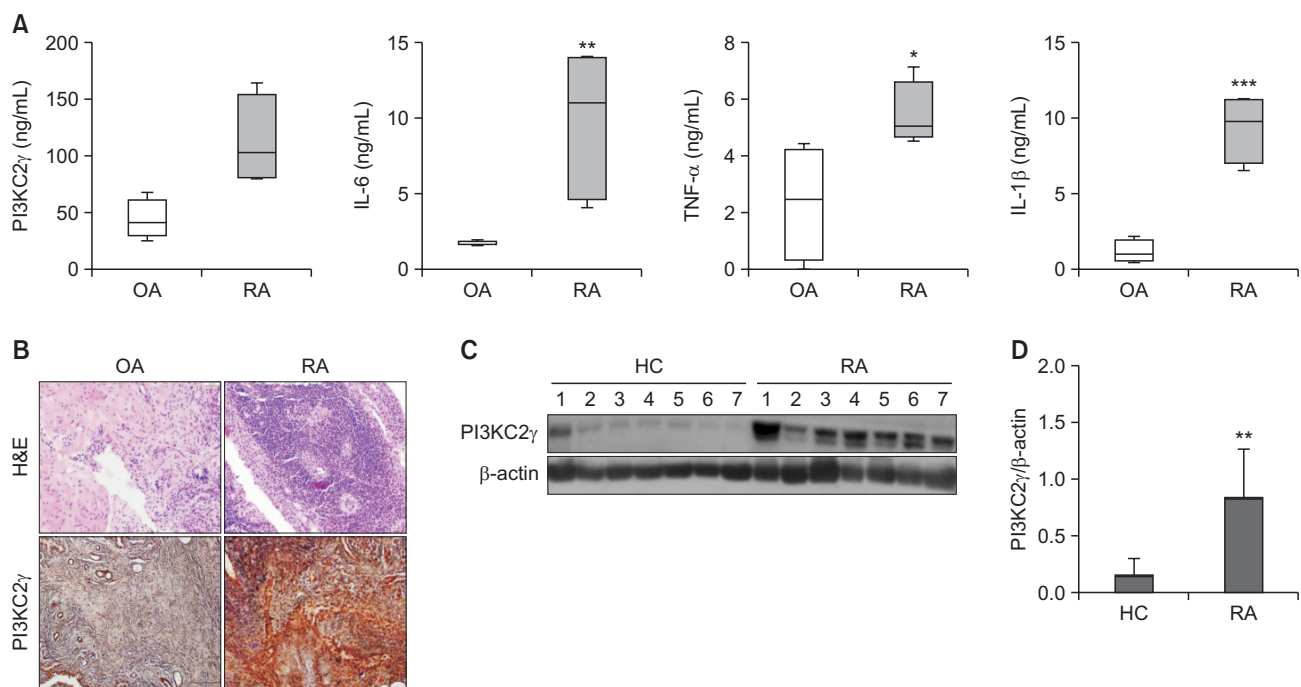


**Fig. 1.** Correlation between inflammation and PI3KC2 $\gamma$  expression. (A) PI3KC2 $\gamma$  and pro-inflammatory cytokines in the synovial fluid of patients with OA (n=9) and RA (n=9) were measured by ELISA. (B) PI3KC2 $\gamma$  expression in the synovial tissue of patients with RA and OA are shown. (C, D) Representative images of western blot analysis of the expression of PI3KC2 $\gamma$  in RA PBMCs (n=7) and HC PBMCs (n=7) are shown. Data represent the mean  $\pm$  SD of densitometric quantification. \* $p < 0.05$ , \*\* $p < 0.01$ , \*\*\* $p < 0.001$ , significance between two groups. OA, osteoarthritis; RA, Rheumatoid arthritis.

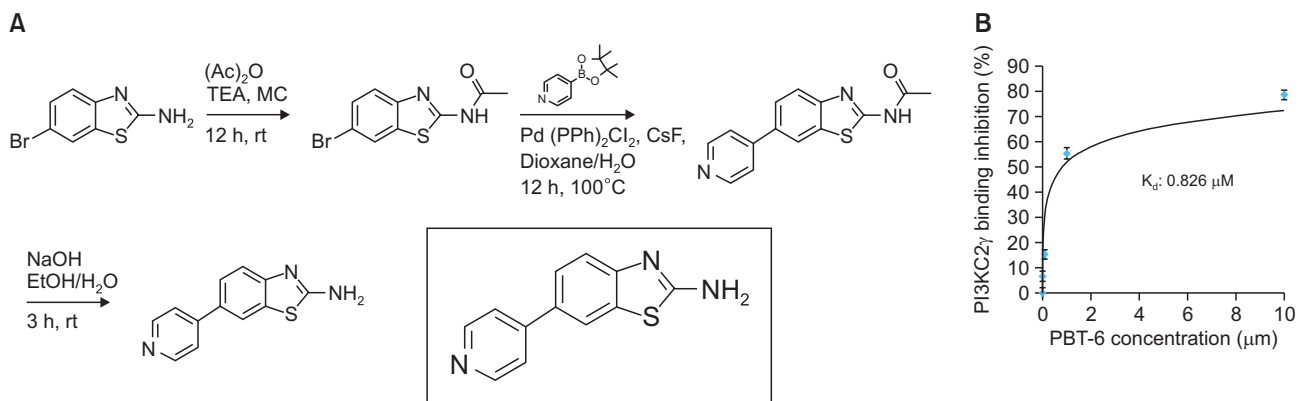


**Fig. 2.** Characterization of PBT-6. (A) Chemical structure of PBT-6. (B) Binding affinity of PBT-6.

medium for 6 h. Cells were then re-suspended in complete media, incubated for 48 h and used for further experiments.

### In vivo CIA model

All animal experiments were performed in accordance with the guidelines of the INHA Institutional Animal Care and Use Committee (INHA IACUC) of the Medical School of Inha University (approval ID: INHA 170718-501). Pathogen-free DBA/1 mice (male, 6 weeks, 20-22 g) were purchased from Orient Bio (Seoul, Korea). The mice were housed under specific pathogen-free conditions with a cycle of 12 h light/12 h dark, a temperature range of  $22 \pm 1^\circ\text{C}$  and  $55 \pm 5\%$  relative humidity. All mice were fed standard laboratory chow and water ad libitum and allowed to acclimatize in our facility for 1 week before any experiments started. For immunization, 200  $\mu\text{g}$  of native bovine type II collagen (Chondrex Inc., Redmond, WA, USA) was mixed with an equal volume of Complete Freund's Adjuvant (Chondrex) by vortexing for 15 min at room temperature. The DBA/1 mice were intradermally immunized in the basal region of the tail with 100  $\mu\text{L}$  of the prepared mixture. On day 21, the mice were boosted with 200  $\mu\text{g}$  of bovine type II collagen in 200  $\mu\text{g}$  Incomplete Freund's Adjuvant (Chondrex). The complete development of CIA was observed 14 days after booster injection. Mice with an arthritis score of 1 or/and 2 were selected and grouped; 20 experimental mice were evenly divided into three groups (group 1, normal control; group 2, vehicle; group 3, 10 mg/kg PBT-6). All mice (except normal control mice) were treated randomly via orally injected with PBT-6 once a day as indicated. The mice were assessed once a week for 40 days after the primary immunization. Paw thickness was measured with a vernier caliper, and arthritis was scored by two independent observers. All four legs of the mice were evaluated and scored from 0 to 4 according to the following scale: (0, no signs of arthritis; 1, redness of the paw or one digit; 2, slight swelling of the ankle or wrist with swelling of limited individual digits; 3, moderate swelling of the ankle or wrist; 4, severe swelling of the entire paw including the digits). AI=the sum of the limb joint swelling grade score (1 grade represented 1 point, the total was 16 points).

### Micro-CT imaging

The mice were anaesthetized with mixture of ketamine (100 mg/kg) and xylazine (2%, 20 mg/kg). Their legs were then excised and fixed in 4% formalin for 2 days. The paws (from the tip of the toes to the end of the distal phalanx) obtained from the experimental mice were scanned, and the images were reconstructed into a three-dimensional structure by micro-CT (SkyScan 1172; Bruker, Kontich, Belgium) with a voxel size of 13.38  $\mu\text{m}$ . The X-ray tube voltage was 59 kV, and the current was 167 mA with a 0.5 mm-thick aluminum filter. The exposure time was 1160 ms. X-ray projections were obtained at  $0.450^\circ$  intervals with a scanning angular rotation of  $180^\circ$ .

### Tartrate-resistant acid phosphatase (TRAP) staining assay

Raw 264.7 cells were cultured in differentiation medium containing 100 ng/ml RANKL and 30 ng/ml M-CSF with varying concentrations of PBT-6 (1-10  $\mu\text{M}$ ) for 6 days. A TRAP staining kit (Sigma-Aldrich) was used to evaluate TRAP expression. TRAP<sup>+</sup> multinucleated cells that contained three or more nuclei were counted as osteoclasts by optical microscopy (Olympus, Tokyo, Japan), and Image Pro Plus (Media Cybernetics, Washington, MD, USA) was used to quantify the

data.

### Transwell migration assay

Macrophage migration assay was established using Transwell-24 units with polycarbonate filters that have a diameter of 6.5 mm and a pore size of 8.0  $\mu\text{m}$  (Corning Costar, Cambridge, MA, USA) according to the manufacturer's instructions. In brief, TNF- $\alpha$ -treated MH7A cells (with or without PBT-6 in growth medium) were cultured in 24-well flat bottom plates. Then, Raw 264.7 cells were starved for 3 h and added to the upper chambers of the Transwell inserts containing LPS in 2% FBS DMEM. A goat anti-mouse CCL2 neutralizing antibody (500 ng/mL) was used with the chemotaxis assay media to determine the biological specificity of the above chemokines produced by the cells to stimulate macrophage migration. After 48 h, the Raw 264.7 cells in the upper compartment were gently wiped away with a cotton swab to remove unmigrated cells, and migrated cells on the underside of the membranes in the Transwell unit were fixed with 20% methanol and stained with 0.2% crystal violet for 30 min. Migrated macrophages were quantified by counting 5 random spots for each sample.

### Immunohistochemistry

Joint tissue samples obtained from CIA mice were decalcified and fixed in 10% buffered formaldehyde at  $4^\circ\text{C}$  overnight. They were embedded in paraffin, and sectioned. Immunostaining was performed on 8 mm sections of joint samples after deparaffinization. Antigen retrieval was performed by incubation with 0.2 mg/mL Proteinase K (Thermo Fisher Scientific,

**Table 1.** Representative PI3kinase profile of PBT-6

Kinase name	POC	Compound Concentration (nM)
EGFR (h)	102	1000
FGFR1 (h)	133	1000
IGF-1R (h)	101	1000
MEK1 (h)	99	1000
MEK2 (h)	101	1000
mTOR (h)	86	1000
PDGFR $\beta$ (h)	106	1000
PKB $\alpha$ (h)	101	1000
PKB $\beta$ (h)	83	1000
PKB $\gamma$ (h)	108	1000
PI3 Kinase (p110a(E542K)/p85a) (h)	87	1000
PI3 Kinase (p110a(H1047R)/p85a) (h)	87	1000
PI3 Kinase (p110a(E545K)/p85a) (h)	89	1000
PI3 Kinase (p110a/p85a) (h)	95	1000
PI3 Kinase (p110a/p65a) (h)	91	1000
PI3 Kinase (p110b/p85a) (h)	89	1000
PI3 Kinase (p110d/p85a) (h)	96	1000
PI3 Kinase (p120g) (h)	66	1000
PI3KC2a (h)	102	1000
PI3KC2g (h)	0	1000

A panel of kinases was tested at 1  $\mu\text{M}$  concentrations in a high-throughput binding assay. Only representative kinases are shown here. Lower percent of control (POC) values represent stronger hits. Values shown are the mean of duplicate measurements.

Grand Island, NY, USA) in PBS for 15 min at room temperature. After gentle washing twice with PBS, endogenous peroxidase was blocked using 0.3% H<sub>2</sub>O<sub>2</sub> in distilled water for 15 min at room temperature. The tissue sections were washed with PBS, blocked with normal goat or horse serum (Vector Laboratories, Burlingame, CA, USA) for 1 h, and incubated at 4°C overnight in 1:50 dilutions of primary antibodies against PI3KC2 $\gamma$  and p-AKT2 (S474). The sections were then incubated with biotinylated secondary antibodies (1:100) for 1 h and visualized with an avidin-biotin-peroxidase complex solution using an ABC kit (Vector Laboratories). Subsequently, they were washed with PBS, developed with a diaminobenzidine tetrahydrochloride (DAB) substrate for 5 min, and counterstained with hematoxylin. At least 3 randomly selected fields for each section were examined at 200 $\times$  magnification.

**Data and statistical analysis**

The data and statistical analysis in this study comply with the recommendations of the British Journal of Pharmacology on experimental design and analysis in pharmacology (Curtis *et al.*, 2015). All the images of western blots and immunohistochemistry staining were quantified using Image J 1.41. All experimental data are presented as mean  $\pm$  SD, and each experiment was performed a minimum of three times. All group data subjected to statistical analysis in the present research have a minimum of n=5 individuals per group or independent samples according to the power analysis in pharmacology (Curtis *et al.*, 2015). Statistical analyses were evaluated using GraphPad Prism 6.0 software (RRID: SCR\_002798, GraphPad, La Jolla, CA, USA). Two groups were compared by analyzed by Student's *t*-test. Three or more different groups were

evaluated by one-way ANOVA. A *p* value of 0.05 or less was regarded as statistically significant.

**RESULTS**

**PI3KC2 $\gamma$  expression in the synovial fluid, synovial tissue, and peripheral blood mononuclear cells (PBMCs) of RA patients**

First, we examined the expression of PI3KC2 $\gamma$  and pro-inflammatory cytokines in the synovial fluid. Analysis of the synovial fluid by ELISA revealed that PI3KC2 $\gamma$  and cytokines such as IL-6, IL-1 $\beta$ , and TNF- $\alpha$  were significantly increased in RA patients compared with osteoarthritis (OA) patients (Fig. 1A). In addition, we evaluated the expression of PI3KC2 $\gamma$  in synovial tissue with histopathologic changes such as noticeable synovial endothelial hyperplasia, granular formation, fibroblast proliferation, vascular proliferation, and severe inflammatory cell infiltration. The expression of PI3KC2 $\gamma$  was markedly increased in the cells of the synovial lining layers and inflammatory infiltrates in the synovial tissue of RA patients compared with OA patients (Fig. 1B). Moreover, the protein level of PI3KC2 $\gamma$  was increased in RA PBMCs compared with healthy control PBMCs (Fig. 1C, 1D). These results demonstrated that PI3KC2 $\gamma$  was increased in the synovial fluid, synovial tissue, and PBMCs of RA patients, indicating that PI3KC2 $\gamma$  is an important regulator of the inflammatory response in RA.

**Discovery of PBT-6, a novel PI3KC2 $\gamma$  inhibitor**

The chemical structure of a novel PI3KC2 $\gamma$  inhibitor, PBT-6, is shown in Fig. 2A. When PBT-6 was subjected to kinase

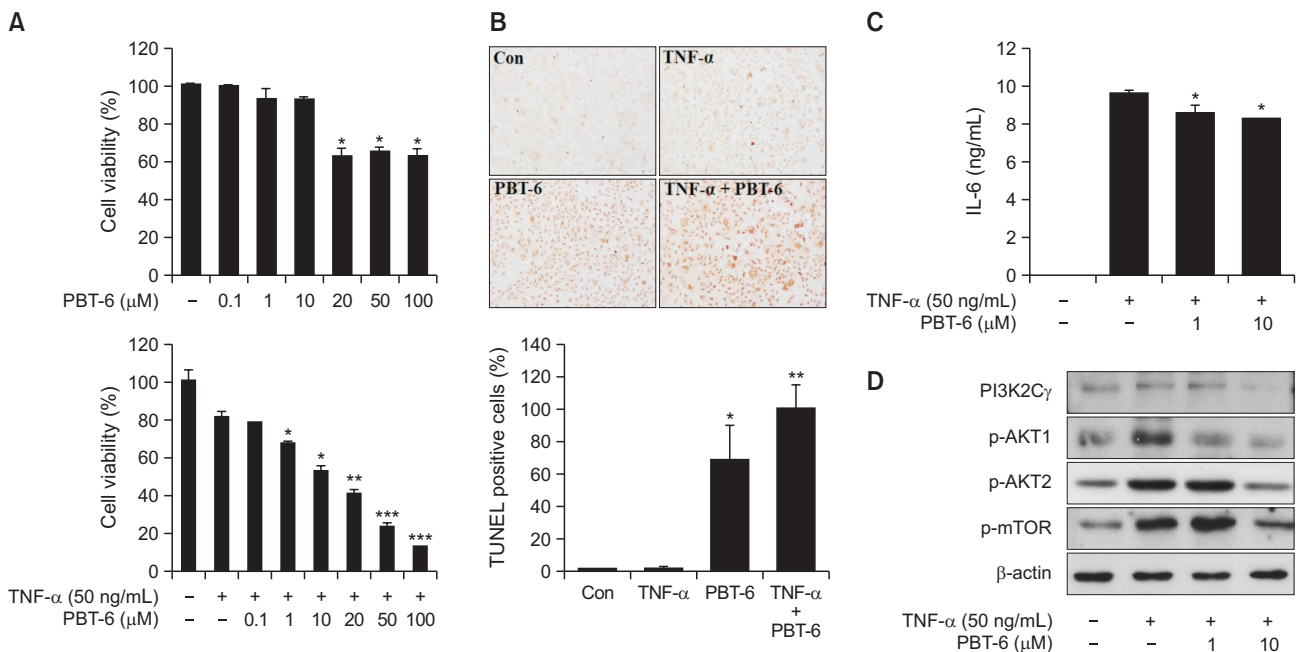


**Fig. 3.** Effect of PBT-6 in TNF- $\alpha$ -induced MH7A cells. (A) TNF- $\alpha$ -mediated MH7A cells were treated with PBT-6 at the indicated concentration for 72 h, and MTT assays were performed. (B) MH7A cells were treated with PBT-6 (10  $\mu$ M) for 24 h after stimulation by TNF- $\alpha$  (50 ng/mL). TUNEL assay were performed. (C) MH7A cells pretreated for 6 h with PBT-6 were stimulated with TNF- $\alpha$  for 24 h. The culture medium was then collected, and the concentration of IL-6 was measured. (D) Cells were pretreated with the PI3KC2 $\gamma$  inhibitor PBT-6 (1 and 10  $\mu$ M) for 6 h and stimulated with TNF- $\alpha$  for 30 min before cell lysis. \**p*<0.05, \*\**p*<0.01, \*\*\**p*<0.001 versus TNF- $\alpha$ -treated cells.

selectivity profiling with a panel of PI3 kinases at 1  $\mu\text{M}$  (Table 1), PBT-6 selectively inhibited PI3KC2 $\gamma$  activity. Next, a homogeneous time-resolved fluorescence (HTRF) kinase assay was performed to measure the binding affinity of PBT-6 to PI3KC2 $\gamma$ . As shown in Fig. 2B, PBT-6 effectively inhibited PI3KC2 $\gamma$  activity, yielding a Kd value of 0.826  $\mu\text{M}$ . Our results indicated that PBT-6 is sufficiently specific to PI3KC2 $\gamma$ .

### Effect of PBT-6 on TNF- $\alpha$ -induced MH7A synovial fibroblasts

Inflammatory cytokines have been identified as key mediators in the pathogenesis of RA (Brennan *et al.*, 1998). Among these cytokines, TNF- $\alpha$  is considered as an essential cytokine for inducing the generation of other inflammatory cytokines in RA (Mukaida *et al.*, 1990). In addition, IL-6 is a master cytokine that is involved in the RA cytokine cascade. Successful anti-cytokine therapies have demonstrated their critical roles in the pathogenesis of RA (Nishimoto *et al.*, 2000; Min *et al.*, 2004). Therefore, we assessed cell viability and measured the IL-6 level in TNF- $\alpha$ -induced synovial fibroblasts (MH7A). When MH7A cells were treated with PBT-6, PBT-6 similarly induced about 40% cell death at 20-100  $\mu\text{M}$  in a dose-independent manner (without TNF- $\alpha$ ). However, PBT-6 increased cell death of TNF- $\alpha$ -induced synovial fibroblasts in dose-dependent manner. In particular, PBT-6 treatment inhibited cell growth by 40-50% at a concentration of 10  $\mu\text{M}$  (Fig. 3A). Cell death of PBT-6 was confirmed by TUNEL assay (Fig. 3B). In addition, PBT-6 significantly decreased the IL-6 level in MH7A cells (Fig. 3C). We also determined whether PBT-6 could inhibit the PI3K/AKT pathway in MH7A cells. As expected, PBT-6 significantly inhibited the phosphorylation of AKT and mTOR, which are key molecules in the PI3K/AKT pathway (Fig. 3D).

### Effect of PBT-6 on LPS-activated Raw 264.7 macrophages

RA is characterized by a massive infiltration of a variety of inflammatory cells including synovial macrophages (Iwamoto *et al.*, 2008). Macrophages are one of the most abundant cell types in the RA synovia and can critically drive the progression of RA (Reddy and Rao, 1976; Burmester *et al.*, 1997). Accordingly, we investigated whether PBT-6 could affect the cell viability of LPS-activated Raw 264.7 macrophages and the secretion of cytokines such as TNF- $\alpha$  and IL-6. When Raw 264.7 macrophages were treated with PBT-6, PBT-6 induced little increase cell death (without TNF- $\alpha$ ). However, PBT-6 increased cell death of LPS-activated macrophages in dose-dependent manner (Fig. 4A), and the secretion of IL-6 and TNF- $\alpha$  was markedly decreased by PBT-6 in LPS-activated Raw 264.7 macrophages (Fig. 4B, 4C). Moreover, PBT-6 significantly inhibited the phosphorylation of AKT and mTOR, indicating that PBT-6 inhibited the secretion of inflammatory cytokines by blocking PI3K/AKT/mTOR signaling.

### Effect of PBT-6 on PI3KC2 $\gamma$ knockdown cells

To better characterize the contribution of PI3KC2 $\gamma$ -mediated PI3K/AKT signaling and to confirm PI3KC2 $\gamma$  targeting of PBT-6, we investigated the changes of PI3K/AKT signaling after silencing PI3KC2 $\gamma$  gene in MHA7 synovial fibroblast and Raw 264.7 macrophage cells. As shown in Fig. 5A, when PI3KC2 $\gamma$  gene was silenced, expression of p-AKT1, p-AKT2, and pan-AKT was decreased in the both cells. Given that expression of AKT1 and AKT2 was similarly low in synovial fibroblast, PI3KC2 $\gamma$  appears to activate PI3K/AKT signaling by affecting both AKT1 and AKT2. Next, we investigated whether PBT-6 is effective in PI3KC2 $\gamma$ -knockdown cells. When PI3KC2 $\gamma$ -silenced MH7A cells were treated with PBT-6, it did not de-

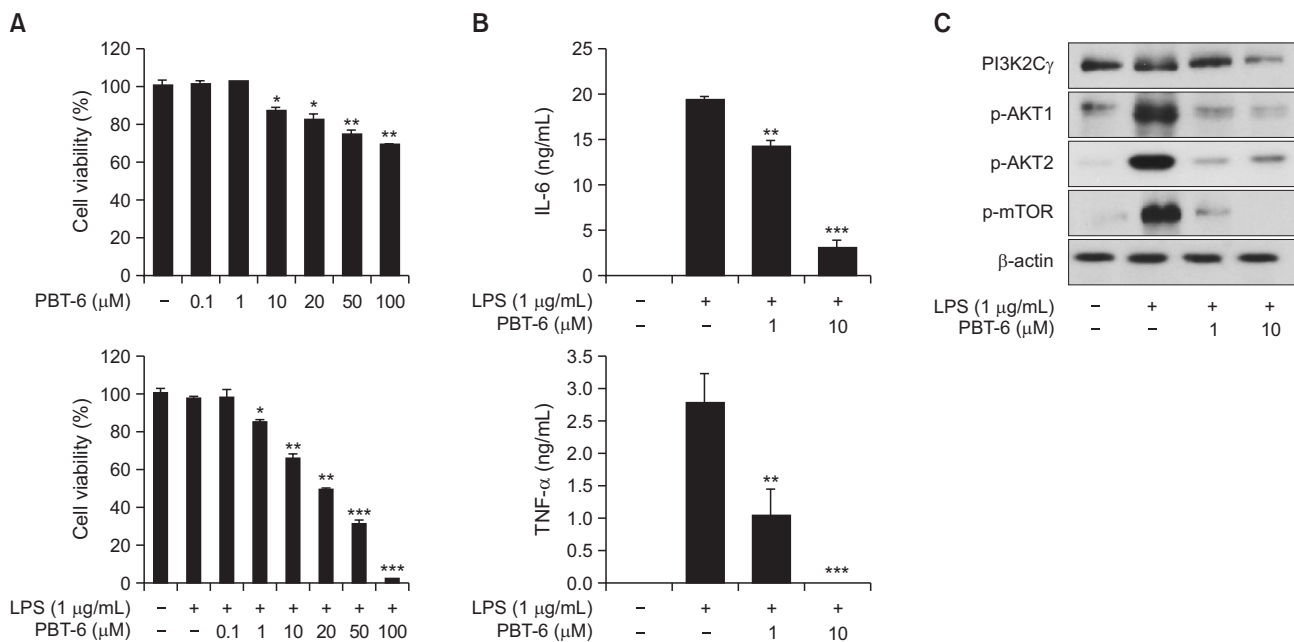


**Fig. 4.** Effect of PBT-6 in LPS-induced Raw 264.7 macrophages. (A) LPS-mediated Raw 264.7 cells were treated with PBT-6 at the indicated concentration for 72 h, and MTT assays were performed. (B, C) Raw 264.7 cells pretreated for 6 h with PBT-6 were stimulated with LPS for 24 h. The culture medium was then collected, and the concentrations of IL-6 and TNF- $\alpha$  were measured. (D) Cells were pretreated with the PI3KC2 $\gamma$  inhibitor PBT-6 (1 and 10  $\mu\text{M}$ ) for 6 h and stimulated with LPS for 30 min before cell lysis. \* $p$ <0.05, \*\* $p$ <0.01, \*\*\* $p$ <0.001 versus LPS-treated cells.

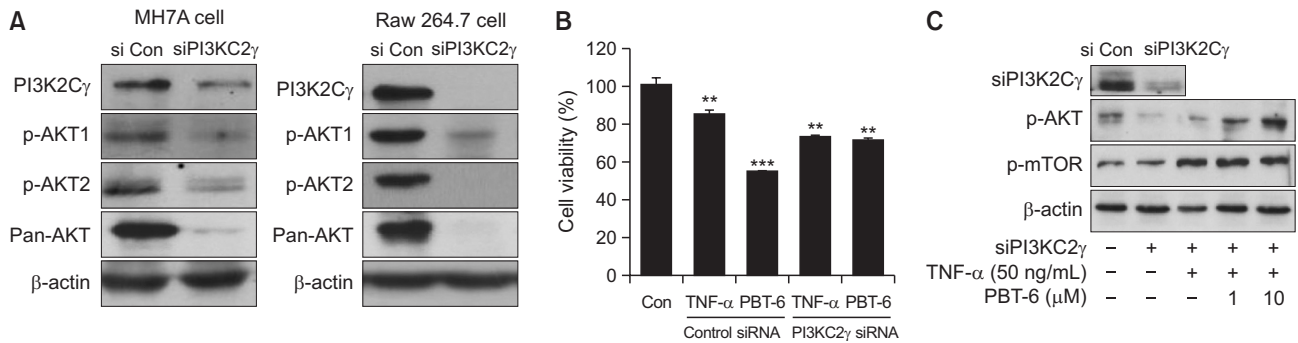


**Fig. 5.** Effect of PBT-6 on PI3KC2 $\gamma$  knockdown cells. (A) PI3K/AKT signaling in PI3KC2 $\gamma$  knockdown cells (MH7A synovial fibroblast and Raw 264.7 macrophages) was examined by Western blot analysis. (B) TNF- $\alpha$ -mediated PI3KC2 $\gamma$  knockdown MH7A cells were treated with PBT-6 (10  $\mu$ M) for 24 h, and MTT assays were performed. (C) PI3KC2 $\gamma$  knockdown cells (MH7A cells) were treated with the PI3KC2 $\gamma$  inhibitor PBT-6 (1 and 10  $\mu$ M) for 6 h and stimulated with LPS (1  $\mu$ g/ml) or TNF- $\alpha$  for 30 min before cell lysis. The values in (B) are the mean  $\pm$  SD (\*\* $p$ <0.01, \*\*\* $p$ <0.001 versus control).

crease cell viability compared to siControl cells (Fig. 5B). Also, when PI3KC2 $\gamma$  was silenced, AKT/mTOR pathway was decreased. However, when this signaling was activated by TNF- $\alpha$  or LPS, PBT-6 did not suppress AKT/mTOR pathway in PI3KC2 $\gamma$ -knockdown cells. From these results, we suggest that PBT-6 shows effects by inhibiting AKT/mTOR signaling via PI3KC2 $\gamma$  binding (Fig. 5C).

**Effect of PBT-6 on migration of macrophages and the osteoclastogenesis**

As macrophages are a major source of cytokines and chemokines, which control the migration and infiltration of monocytes/macrophages into the inflamed synovium (Burmester *et al.*, 1997), we investigated whether PBT-6 could inhibit macrophage migration to synovial fibroblasts with chemotaxis by Transwell chamber assay. The migration of activated macrophages was suppressed by PBT-6 (10  $\mu$ M) treatment in the conditioned medium of TNF- $\alpha$ -induced synovial fibroblasts (bottom plate) (Fig. 6A). CCL2 is a key regulator in monocyte migration such as macrophage and the inflammatory response during RA pathogenesis (Koch *et al.*, 1992). Thus, we identified whether PBT-6 could inhibit macrophage migration via CCL2. For this experiment, we used CCL2 neutralizing antibody. An *in vitro* chemotaxis assay revealed that macrophage migration in response to synovial fibroblast was attenuated by incubation with an anti-CCL2 neutralizing antibody (Fig. 6B). Also, PBT-6 inhibited macrophage migration to synovial fibroblasts (Fig. 6A). However, PBT-6 did not inhibit macrophage migration after treatment of CCL2 neutralizing antibody (Fig. 6B). These results imply that inhibition of macrophage migration by PBT-6 may be blocked *via* regulation of CCL2 inhibition.

Inflammation is known to increase osteoclastogenesis in RA. In addition, cytokines such as TNF- $\alpha$  and IL-6 (which are osteoclastogenic) can promote osteoclastic bone resorption (Weitzmann *et al.*, 2000). Also, the migrated synovial macrophage highly induced osteoclast differentiation. Given that PBT-6 decreased the production of TNF- $\alpha$  and IL6 in macrophages and synovial fibroblasts and decreased macrophage migration to synovial fibroblasts, we hypothesized that PBT-6 could inhibit osteoclastogenesis. To determine the effects of PBT-6 on osteoclastogenesis, the formation of osteoclast cells from Raw 264.7 macrophages was induced by the addition of

RANKL (100 ng/mL). Cells in the control group were successfully differentiated into mature TRAP-positive multinucleated osteoclasts, and PBT-6 effectively reduced the formation of TRAP-positive osteoclasts (Fig. 6C, \*\*\* $p$ <0.01). The RANKL receptor (RANK) to nuclear factor of activated T cells c1 (NFATc1) is known as the transcription factor most strongly induced by RANKL stimulation in the early phase of differentiation into osteoclasts, which regulates several genes required for osteoclastic differentiation (Asagiri *et al.*, 2005). As shown in Fig. 6D, a significant increase in NFATc1 expression was observed in RANKL-stimulated Raw 264.7 cells, which was inhibited by PBT-6.

**PBT-6 attenuates arthritis severity in mice with CIA**

Considering the *in vitro* findings, the therapeutic effect of PBT-6 was evaluated in mice with CIA. As shown in Fig. 7A, PBT-6 attenuated the swelling, erythema, and joint rigidity of the paws of mice with CIA. In addition, arthritis scores were significantly lower in the PBT-6-treated group (oral injection of 10 mg/kg PBT-6) than in the vehicle-treated group (oral injection of 0.5% methyl cellulose) (Fig. 7B). Furthermore, paw thickness was measured to analyze the beneficial effect of PBT-6; the results were correlated with arthritis scores (Fig. 7C). Serum cytokine analysis demonstrated that TNF- $\alpha$  and IL-6 were significantly lower in the PBT-6-treated group than in the vehicle-treated group (Fig. 7D). Histopathologic evaluation revealed severe synovial inflammation, synovial hyperplasia, cartilage damage, pannus formation, and bone erosion in mice with CIA. In contrast, the ankle joints in the PBT-6-treated group showed great improvements (Fig. 7E). Consistently, histological scores revealed that synovial inflammation, cartilage destruction, and bone destruction were significantly attenuated by PBT-6 treatment in mice with CIA (Fig. 7F). Furthermore, PI3KC2 $\gamma$  and p-AKT2 were highly expressed in inflamed cells around the joints of CIA mice, but PBT-6 treatment inhibited their expression (Fig. 7E). When we analyzed bone changes by three-dimensional micro-computed tomography, characteristic changes such as articular destruction, joint displacement, and irregular bone proliferation were observed in mice with CIA, and PBT-6 treatment alleviated bone destruction and increased bone volume, bone mineral density, and trabecular thickness (Fig. 8).

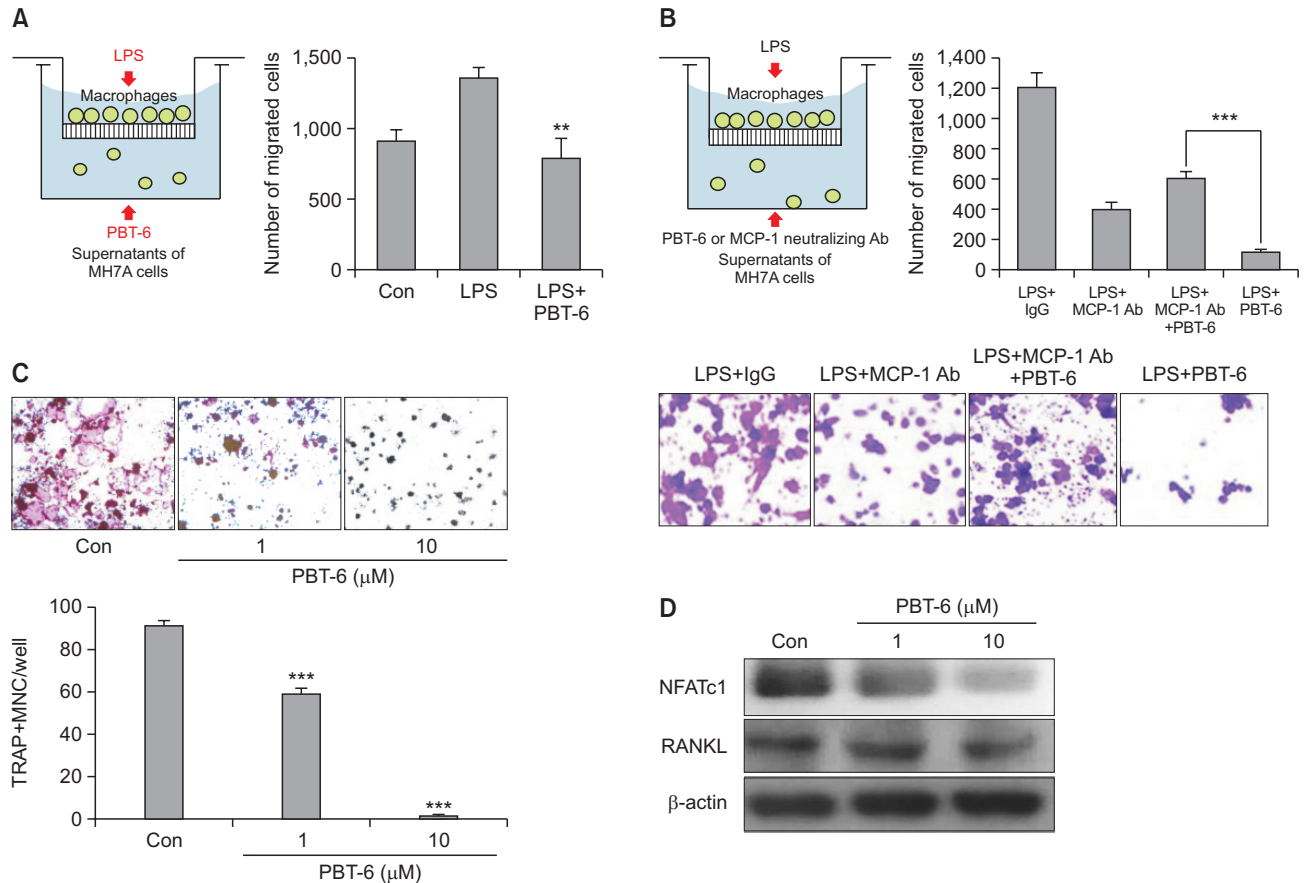


**Fig. 6.** Effect of PBT-6 on macrophage migration and osteoclastogenesis. (A) Raw 264.7 cell migration was assayed using 24-well Transwell inserts. MH7A synovial fibroblast cells became inflammation condition by TNF- $\alpha$  (100 ng/mL) treatment for 24 h. After collection of condition media (CM) of MH7A cells, CM was added to lower chambers of the Transwell and PBT-6 (10  $\mu$ M) was treated into CM. Then, Raw 264.7 cells were starved for 3 h and added to the upper chambers of the Transwell inserts containing 1  $\mu$ g/mL LPS for 48 h in 2% FBS DMEM (\*\* $p$ <0.01 versus LPS-treated cells). (B) CM of synovial fibroblast MH7A cells was added to lower chambers of the Transwell and CCL2 neutralizing antibody (Ab, 500 ng/mL), IgG Ab, or/and PBT-6 (10  $\mu$ M) was treated into CM. Then, Raw 264.7 cells were starved for 3 h and added to the upper chambers of the Transwell inserts containing 1  $\mu$ g/ml LPS for 48 h (\*\* $p$ <0.001). (C) The osteoclastogenesis of Raw 264.7 cells was induced by RANKL (100 ng/mL) and M-CSF (30 ng/mL) in the presence or absence of PBT-6 for 6 days. Multinucleated osteoclasts were counted after TRAP staining. Data represent the mean  $\pm$  SD of three independent experiments (\*\* $p$ <0.001 versus control). (D) Raw 264.7 cells were pretreated with PBT-6 (1 and 10  $\mu$ M) for 1 h and treated with RANKL (100 ng/mL) and M-CSF (30 ng/mL) in the presence or absence of PBT-6 for 24 h. NFATc1 and RANKL were detected with specific antibodies.

## DISCUSSION

PI3K $\gamma$  has been reported to be involved in immune response activation and inflammation in RA. However, little is known about the involvement of PI3K $2\gamma$  in RA. In the present study, we demonstrate for the first time the up-regulation of PI3K $2\gamma$  in patients with RA and its association with inflammation and disease activity. The novel findings in our study indicate that PI3K $2\gamma$  could be a therapeutic target for RA and that PBT-6 (a PI3K $2\gamma$  inhibitor) could suppress arthritis progression *in vitro* and *in vivo*.

PI3Ks are interesting targets for the modulation of inflammatory diseases (Wetzker and Rommel, 2004), which are divided into class I, II, and III (Yu *et al.*, 1998). The PI3K $1\alpha$  and C1 $\beta$  isoforms regulate a variety of cell functions including survival and proliferation, whereas the PI3K $1\delta$  and C1 $\gamma$  isoforms regulate immune responses (Katso *et al.*, 2001). On the other hand, class II PI3Ks are composed of three isoforms,

PI3K $2\alpha$ , PI3K $2\beta$ , and PI3K $2\gamma$  (Wymann and Pirola, 1998; Foster *et al.*, 2003). Among these isoforms, PI3K $2\gamma$  has a much more restricted tissue distribution than PI3K $2\alpha$  and PI3K $2\beta$ , being generally localized in exocrine glands. High levels of PI3K $2\gamma$  are found in the liver (specifically in the hepatic parenchyma), breast, prostate, and salivary gland (Ho *et al.*, 1997). A previous study on PI3K $2\gamma$  found that its expression is increased following partial hepatectomy, suggesting that PI3K $2\gamma$  may play a role in the maturation of hepatic cells (Lloyd and Deakin, 1975). In our study, the high expression of PI3K $2\gamma$  was confirmed in the liver, and there was no difference in its expression between RA and normal livers. However, the levels of PI3K $2\gamma$  in the synovial tissue and fluid of RA patients were significantly increased, indicating that PI3K $2\gamma$  may be a possible exacerbating factor of RA.

In contrast to class I PI3Ks, there are limited studies on isoform-specific inhibitors for class II PI3Ks including PI3K $2\gamma$ . Moreover, class II PI3Ks respond poorly to class I PI3K inhibi-



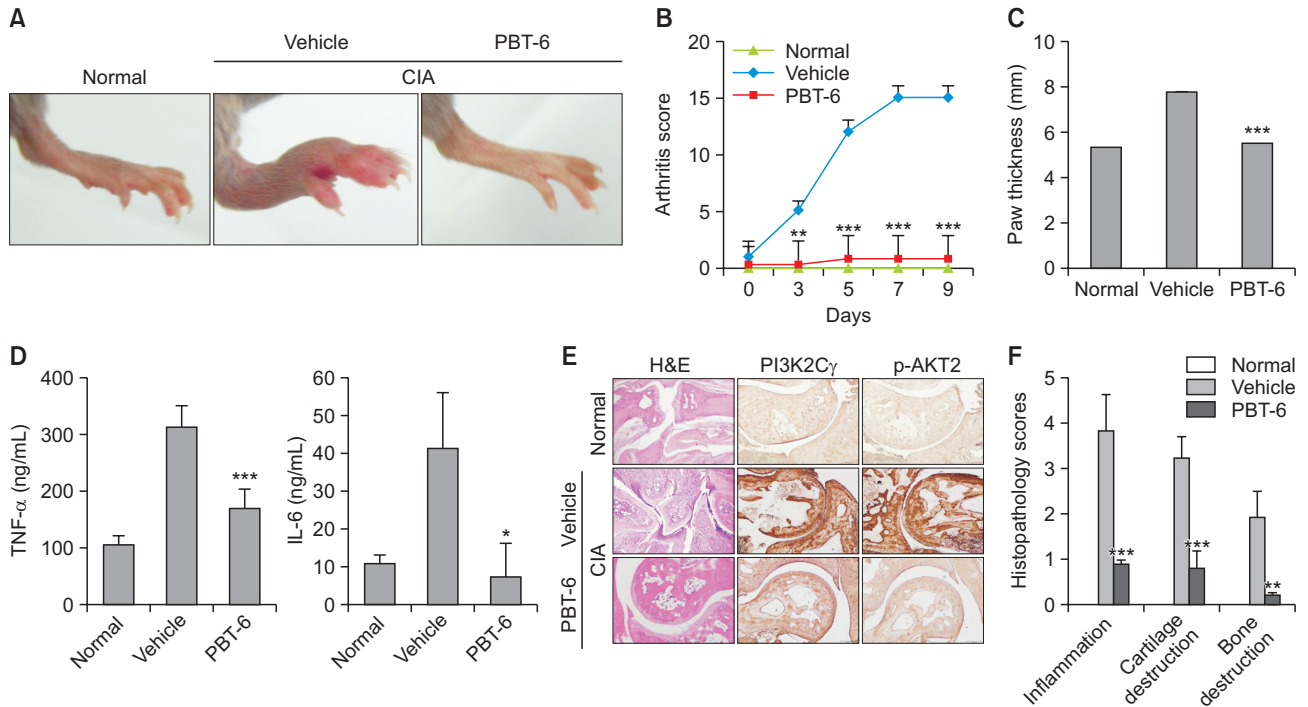


**Fig. 7.** Effect of PBT-6 in mice with CIA. (A) Representative photographs of the hind paws on day 40 are shown (n=5). (B, C) The effect of PBT-6 on the clinical score and paw thickness of mice with CIA was evaluated. The values in B and C are the mean ± SD (\*\*p<0.01, \*\*\*p<0.001 versus vehicle). (D) The effect of PBT-6 on the serum levels of TNF-α and IL-6 in mice with CIA was evaluated using ELISA. The values are the mean ± SD (\*p<0.05, \*\*\*p<0.001 versus vehicle). (E) Specimens of the removed arthritic paws were stained with H&E and IHC (original magnification 100×). (F) Histopathological scores including inflammation, cartilage, and bone destruction were analyzed by two independent pathologists (\*\*p<0.01, \*\*\*p<0.001 versus vehicle).

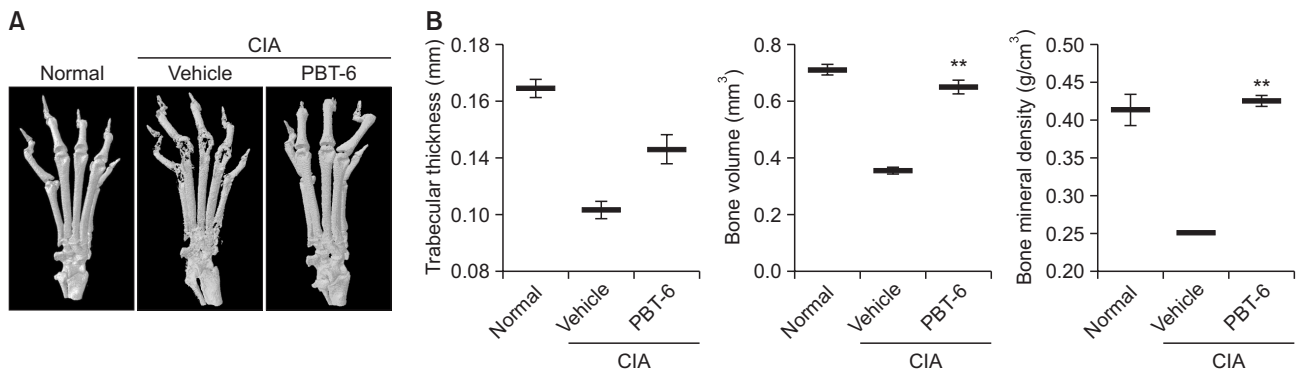


**Fig. 8.** Effect of PBT-6 on bone characteristics in mice with CIA. (A) Severe bone erosion was observed in the hind paws of CIA mice (n=5). (B) Bone volume, trabecular thickness, and bone mineral density were quantified. The values are the mean ± SD (\*\*p<0.01 versus vehicle).

tors, and this has hindered the functional studies of this class of PI3K (O’Farrell *et al.*, 2013). Given that PI3KC2γ was significantly increased in the synovial tissue and fluid of RA patients in our study, we hypothesized that the pharmacological blockade of PI3KC2γ might offer an innovative rationale-based therapeutic strategy for RA. Therefore, we developed PBT-6, a potent and isoform-selective PI3KC2γ inhibitor for RA treatment, and evaluated its effects. In the present study, we demonstrated that PBT-6 effectively ameliorated arthritis in mice with CIA. Histological analysis and micro-CT further confirmed that synovial inflammation, cartilage destruction, pannus for-

mation, and bone destruction were significantly attenuated by PBT-6 treatment. In CIA mice, various cytokines, especially pro-inflammatory cytokines, play crucial roles in activating immune and inflammatory cells, which would favor the induction of autoimmunity, chronic inflammation, and subsequent joint destruction (McInnes and Schett, 2007). Our results show that treatment with PBT-6 significantly suppressed the systemic levels of pro-inflammatory cytokines such as TNF-α and IL-6 *in vitro* and *in vivo*.

In RA, synovial fibroblasts are a key component of the invasive rheumatoid synovium and play an important role in

the initiation and perpetuation of destructive joint inflammation (Huber *et al.*, 2006; Bottini and Firestein, 2013). TNF- $\alpha$  is a predominant pro-inflammatory cytokine associated with RA and can stimulate the proliferation of synovial fibroblasts and increase the production of inflammatory mediators (Kappoor *et al.*, 2011). In addition, IL-6 and IL-1 $\beta$  are downstream mediators of TNF- $\alpha$ , which together play a critical role in mediating synovitis and joint destruction in RA (Zheng *et al.*, 2014). Therefore, TNF- $\alpha$  has been widely used to mimic arthritis *in vitro* studies (Rosengren *et al.*, 2012; Jia *et al.*, 2015). To further explore the possible pharmacological mechanism of PBT-6 in RA treatment, we investigated the effects of PBT-6 in TNF- $\alpha$ -induced human synovial fibroblasts (MH7A). The results showed that PBT-6 increased the cell death of TNF- $\alpha$ -induced human synovial fibroblasts and inhibited the level of IL-6. A recent study reported that PI3KC2 $\gamma$  could selectively control endosomal AKT2 activation on insulin signaling in liver (Braccini *et al.*, 2015); thus, we investigated whether PBT-6 could inhibit the expression of AKT2 as well as AKT1 and mTOR (its downstream target) in synovial fibroblasts. PBT-6 effectively inhibited the PI3K signaling pathway activated by TNF- $\alpha$  *via* the suppression of the expression of AKT1, AKT2, and mTOR (its downstream target). Indeed, when PI3KC2 $\gamma$  gene was silenced, activation of both AKT1 and AKT2 was decreased in synovial cells. PI3KC2 $\gamma$  appears to activate PI3K/AKT signaling by affecting both AKT1 and AKT2. When PI3KC2 $\gamma$  gene was silenced, the decrease of p-AKT expression by PBT-6 did not observed in TNF-induced synovial fibroblast. Collectively, we suggest that PBT-6 could inhibit PI3K/AKT signaling by targeting PI3KC2 $\gamma$ , thereby reducing the inflammatory response in synovial fibroblasts.

In addition to synovial fibroblasts, our study revealed that PBT-6 affected the activation and migration of macrophages. In RA, macrophages are the key effector cells in the acute and chronic phases by secreting pro-inflammatory cytokines and mediators that drive the infiltration of immune cells, cartilage damage, and bone destruction (Clavel *et al.*, 2016). The number of synovial macrophages is positively correlated with disease severity such as the degree of joint damage (Mulherin *et al.*, 1996). A change in synovial macrophages is a sensitive biomarker of the response to anti-rheumatic treatment in patients with RA (Haringman *et al.*, 2005). In addition, emerging evidence suggests that the cell death of activated macrophages is an important mechanism for controlling inflammation (Tabas, 2010). In our study, PBT-6 increased the cell death of activated macrophages and further inhibited macrophage migration to synovial fibroblasts and TNF- $\alpha$  release, resulting in the reduction of inflammation in RA. Additionally, as CCL2 is one of the key factors involved in the initiation of inflammation, which triggers chemotaxis and migration of monocytes to inflammatory lesions, we identified whether PBT-6 inhibited macrophage migration *via* CCL2. Interestingly, when CCL2 was neutralized by its antibody, PBT-6 did not inhibit macrophage migration. These results imply that inhibition of macrophage migration by PBT-6 is blocked *via* regulation of CCL2.

Until now, little is known about the role of PI3KC2 $\gamma$  in inflammation. Only, Rozycka *et al.* have reported that PI3KC2 $\gamma$  may be involved in immune cells signaling such as iCOS-iCOSL signaling and natural killing cells signaling from genomic sequencing data (Rasmussen *et al.*, 2012). Also, Yu *et al.* (2010) have reported that knockdown of PI3KC2 $\gamma$  suppressed the activated chemotaxis in leukemia cells. Considering our results

for the role of PI3KC2 $\gamma$  in RA, the PBT6, a PI3KC2 $\gamma$  inhibitor might suppress macrophage activation and its migration to synovial fibroblast *via* CCL2. From our results, we suggest that PBT-6 may be effectively involved in immune cells response such as macrophage *via* regulation of PI3KC2 $\gamma$  in inflammatory condition of RA.

Osteoclasts are multinucleated giant cells with the capacity to resorb mineralized tissues. They are derived from hematopoietic progenitors of the monocyte-macrophage lineage (Udagawa, 2003). Among osteoclastogenic factors, RANK is expressed on the surface of hematopoietic osteoclast progenitors that belong to the monocyte/macrophage lineage, thereby altering the RANK/RANKL/OPG system, which is the final regulator of bone resorption (Takayanagi *et al.*, 2000; Hofbauer and Heufelder, 2001; Romas *et al.*, 2002). In arthritis, osteoclast precursors that express RANK recognize RANKL and differentiate into osteoclasts (Jones *et al.*, 2002). In addition, TNF- $\alpha$  and IL-6 are representative osteoclastogenic cytokines that promote bone resorption by osteoclasts (Weitzmann *et al.*, 2000). In particular, these cytokines can increase osteoclast function in cooperation with RANKL (Vitale and Ribeiro Fde, 2007). Recently, TNF- $\alpha$  and IL-6 have been reported to synergistically induce osteoclast-like cells and increase bone resorption activity (Yokota *et al.*, 2014). In this study, as PBT-6 reduced the levels of TNF- $\alpha$  and IL-6 and the migration and activation of macrophages, we investigated whether PBT-6 could inhibit osteoclastogenesis. PBT-6 significantly inhibited the osteoclastic differentiation of RANKL-induced macrophages. Moreover, it decreased the expression of RANKL-induced osteoclastogenic marker genes such as TRAP and NFATc, thus demonstrating its anti-osteoclastogenic capacity. This effect was confirmed by micro-CT showing that PBT-6 significantly attenuated cartilage and bone destruction in mice with CIA. Based on the results, the anti-osteoclastogenic effect of PBT-6 may be attributed to the regulation of RANKL/RANK signaling by suppressing cytokines such as TNF- $\alpha$  and IL-6 with a protective mechanism against joint inflammation and bone destruction.

In conclusion, our data demonstrate that PI3KC2 $\gamma$  could be a therapeutic target for RA, which was significantly increased in the synovial fluid and tissue of RA patients. PBT-6, a selective PI3KC2 $\gamma$  inhibitor, improved RA symptoms and severity *in vivo* and *in vitro* by inhibiting osteoclastogenesis and cytokine production *via* the suppression of macrophage activation and migration. These results suggest that PBT-6 may exert a beneficial effect as a novel PI3KC2 $\gamma$  inhibitor in the treatment of RA.

## CONFLICT OF INTEREST

The authors declare that they have no competing interests.

## ACKNOWLEDGMENTS

This research was supported by the Bio & Medical Technology Development Program of the National Research Foundation (NRF) & funded by the Korean government (MSIT) (No. 2019M3E5D1A02069621) and Inha University Grant, Korea.

## REFERENCES

- Asagiri, M., Sato, K., Usami, T., Ochi, S., Nishina, H., Yoshida, H., Morita, I., Wagner, E. F., Mak, T. W., Serfling, E. and Takayanagi, H. (2005) Autoamplification of NFATc1 expression determines its essential role in bone homeostasis. *J. Exp. Med.* **202**, 1261-1269.
- Bottini, N. and Firestein, G. S. (2013) Duality of fibroblast-like synoviocytes in RA: passive responders and imprinted aggressors. *Nat. Rev. Rheumatol.* **9**, 24-33.
- Boyle, D. L., Kim, H. R., Topolewskim, K., Bartok, B. and Firestein, G. S. (2014) Novel phosphoinositide 3-kinase  $\delta,\gamma$  inhibitor: potent anti-inflammatory effects and joint protection in models of rheumatoid arthritis. *J. Pharmacol. Exp. Ther.* **348**, 271-280.
- Braccini, L., Ciraolo, E., Campa, C. C., Perino, A., Longo, D. L., Tibolla, G., Pregolato, M., Cao, Y., Tassone, B., Damilano, F., Lafargue, M., Calautti, E., Falasca, M., Norata, G. D., Backer, J. M. and Hirsch, E. (2015) PI3K-C2gamma is a Rab5 effector selectively controlling endosomal Akt2 activation downstream of insulin signalling. *Nat. Commun.* **6**, 7400.
- Brennan, F. M., Maini, R. N. and Feldmann, M. (1998) Role of pro-inflammatory cytokines in rheumatoid arthritis. *Springer Semin. Immunopathol.* **20**, 133-147.
- Burmester, G. R., Stuhlmüller, B., Keyszer, G. and Kinne, R. W. (1997) Mononuclear phagocytes and rheumatoid synovitis. Mastermind or workhorse in arthritis? *Arthritis Rheum.* **40**, 5-18.
- Camps, M., Ruckle, T., Ji, H., Ardisson, V., Rintelen, F., Shaw, J., Ferrandi, C., Chabert, C., Gillieron, C., Françon, B., Martin, T., Gretenier, D., Perrin, D., Leroy, D., Vitte, P. A., Hirsch, E., Wymann, M. P., Cirillo, R., Schwarz, M. K. and Rommel, C. (2005) Blockade of PI3Kgamma suppresses joint inflammation and damage in mouse models of rheumatoid arthritis. *Nat. Med.* **11**, 936-943.
- Clavel, C., Ceccato, L., Anquetil, F., Serre, G. and Sebbag, M. (2016) Among human macrophages polarised to different phenotypes, the M-CSF-oriented cells present the highest pro-inflammatory response to the rheumatoid arthritis-specific immune complexes containing ACPA. *Ann. Rheum. Dis.* **75**, 2184-2191.
- Curtis, M. J., Bond, R. A., Spina, D., Ahluwalia, A., Alexander, S. P., Giembycz, M. A., Gilchrist, A., Hoyer, D., Insel, P. A., Izzo, A. A., Lawrence, A. J., MacEwan, D. J., Moon, L. D., Wonnacott, S., Weston, A. H. and McGrath, J. C. (2015) Experimental design and analysis and their reporting: new guidance for publication in BJP. *Br. J. Pharmacol.* **172**, 3461-3471.
- Del Prete, A., Vermi, W., Dander, E., Otero, K., Barberis, L., Luini, W., Bernasconi, S., Sironi, M., Santoro, A., Garlanda, C., Facchetti, F., Wymann, M. P., Vecchi, A., Hirsch, E., Mantovani, A. and Sozzani, S. (2004) Defective dendritic cell migration and activation of adaptive immunity in PI3Kgamma-deficient mice. *EMBO J.* **23**, 3505-3515.
- Divecha, N. and Irvine, R. F. (1995) Phospholipid signaling. *Cell* **80**, 269-278.
- Foster, F. M., Traer, C. J., Abraham, S. M. and Fry, M. J. (2003) The phosphoinositide (PI) 3-kinase family. *J. Cell Sci.* **116**, 3037-3040.
- Freitag, A., Prajwal, P., Shymanets, A., Harteneck, C., Nürnberg, B., Schächtele, C., Kubbutat, M., Totzke, F. and Laufer, S. A. (2015) Development of first lead structures for phosphoinositide 3-kinase-C2gamma inhibitors. *J. Med. Chem.* **58**, 212-221.
- Frisell, T., Baecklund, E., Bengtsson, K., Di Giuseppe, D., Forsblad d'Elia, H. and Askling, J.; ARTIS Study group (2018) Patient characteristics influence the choice of biological drug in RA, and will make non-TNFi biologics appear more harmful than TNFi biologics. *Ann. Rheum. Dis.* **77**, 650-657.
- Gillespie, J., Savic, S., Wong, C., Hemphshall, A., Inman, M., Emery, P., Grigg, R. and McDermott, M. F. (2012) Histone deacetylases are dysregulated in rheumatoid arthritis and a novel histone deacetylase 3-selective inhibitor reduces interleukin-6 production by peripheral blood mononuclear cells from rheumatoid arthritis patients. *Arthritis Rheum.* **64**, 418-422.
- Haringman, J. J., Gerlag, D. M., Zwinderman, A. H., Smeets, T. J., Kraan, M. C., Baeten, D., McInnes, I. B., Bresnihan, B. and Tak, P. P. (2005) Synovial tissue macrophages: a sensitive biomarker for response to treatment in patients with rheumatoid arthritis. *Ann. Rheum. Dis.* **64**, 834-838.
- Harris, S. J., Foster, J. G. and Ward, S. G. (2009) PI3K isoforms as drug targets in inflammatory diseases: lessons from pharmacological and genetic strategies. *Curr. Opin. Investig. Drugs* **10**, 1151-1162.
- Hirsch, E., Katanaev, V. L., Garlanda, C., Azzolino, O., Pirola, L., Silengo, L., Sozzani, S., Mantovani, A., Altruda, F. and Wymann, M. P. (2000) Central role for G protein-coupled phosphoinositide 3-kinase gamma in inflammation. *Science* **287**, 1049-1053.
- Ho, L. K., Liu, D., Rozycka, M., Brown, R. A. and Fry, M. J. (1997) Identification of four novel human phosphoinositide 3-kinases defines a multi-isoform subfamily. *Biochem. Biophys. Res. Commun.* **235**, 130-137.
- Hofbauer, L. C. and Heufelder, A. E. (2001) The role of osteoprotegerin and receptor activator of nuclear factor kappaB ligand in the pathogenesis and treatment of rheumatoid arthritis. *Arthritis Rheum.* **44**, 253-259.
- Huber, L. C., Distler, O., Tamer, I., Gay, R. E., Gay, S. and Pap, T. (2006) Synovial fibroblasts: key players in rheumatoid arthritis. *Rheumatology (Oxford)* **45**, 669-675.
- Iwamoto, T., Okamoto, H., Toyama, Y. and Momohara, S. (2008) Molecular aspects of rheumatoid arthritis: chemokines in the joints of patients. *FEBS J.* **275**, 4448-4455.
- Jia, Q., Cheng, W., Yue, Y., Hu, Y., Zhang, J., Pan, X., Xu, Z. and Zhang, P. (2015) Cucurbitacin E inhibits TNF- $\alpha$ -induced inflammatory cytokine production in human synoviocyte MH7A cells via suppression of PI3K/Akt/NF- $\kappa$ B pathways. *Int. Immunopharmacol.* **29**, 884-890.
- Jones, D. H., Kong, Y. Y. and Penninger, J. M. (2002) Role of RANKL and RANK in bone loss and arthritis. *Ann. Rheum. Dis.* **61 Suppl 2**, ii32-ii39.
- Kapoor, M., Martel-Pelletier, J., Lajeunesse, D., Pelletier, J. P. and Fahmi, H. (2011) Role of proinflammatory cytokines in the pathophysiology of osteoarthritis. *Nat. Rev. Rheumatol.* **7**, 33-42.
- Katso, R., Okkenhaug, K., Ahmadi, K., White, S., Timms, J. and Waterfield, M. D. (2001) Cellular function of phosphoinositide 3-kinases: implications for development, homeostasis, and cancer. *Annu. Rev. Cell Dev. Biol.* **17**, 615-675.
- Kim, D. I., Kim, S. R., Kim, H. J., Lee, S. J., Lee, H. B., Park, S. J., Im, M. J. and Lee, Y. C. (2012) PI3K- $\gamma$  inhibition ameliorates acute lung injury through regulation of I $\kappa$ B $\alpha$ /NF- $\kappa$ B pathway and innate immune responses. *J. Clin. Immunol.* **32**, 340-351.
- Koch, A. E., Kunkel, S. L., Harlow, L. A., Johnson, B., Evanoff, H. L., Haines, G. K., Burdick, M. D., Pope, R. M. and Strieter, R. M. (1992) Enhanced production of monocyte chemoattractant protein-1 in rheumatoid arthritis. *J. Clin. Invest.* **90**, 772-779.
- Li, Z., Jiang, H., Xie, W., Zhang, Z., Smrcka, A. V. and Wu, D. (2000) Roles of PLC-beta2 and -beta3 and PI3Kgamma in chemoattractant-mediated signal transduction. *Science* **287**, 1046-1049.
- Lloyd, G. and Deakin, H. G. (1975) Phobias complicating treatment of uterine carcinoma. *Br. Med. J.* **4**, 440.
- McInnes, I. B. and Schett, G. (2007) Cytokines in the pathogenesis of rheumatoid arthritis. *Nat. Rev. Immunol.* **7**, 429-442.
- McInnes, I. B. and Schett, G. (2011) The pathogenesis of rheumatoid arthritis. *N. Engl. J. Med.* **365**, 2205-2219.
- Min, D. J., Cho, M. L., Lee, S. H., Min, S. Y., Kim, W. U., Min, J. K., Park, S. H., Cho, C. S. and Kim, H. Y. (2004) Augmented production of chemokines by the interaction of type II collagen-reactive T cells with rheumatoid synovial fibroblasts. *Arthritis Rheum.* **50**, 1146-1155.
- Mukaida, N., Mahe, Y. and Matsushima, K. (1990) Cooperative interaction of nuclear factor-kappa B- and cis-regulatory enhancer binding protein-like factor binding elements in activating the interleukin-8 gene by pro-inflammatory cytokines. *J. Biol. Chem.* **265**, 21128-21133.
- Mulherin, D., Fitzgerald, O. and Bresnihan, B. (1996) Synovial tissue macrophage populations and articular damage in rheumatoid arthritis. *Arthritis Rheum.* **39**, 115-124.
- Nishimoto, N., Kishimoto, T. and Yoshizaki, K. (2000) Anti-interleukin 6 receptor antibody treatment in rheumatic disease. *Ann. Rheum. Dis.* **59 Suppl 1**, i21-i27.
- O'Farrell, F., Rustenm, T. E. and Stenmark, H. (2013) Phosphoinositide 3-kinases as accelerators and brakes of autophagy. *FEBS J.* **280**, 6322-6337.

- Pap, T. and Korb-Pap, A. (2015) Cartilage damage in osteoarthritis and rheumatoid arthritis—two unequal siblings. *Nat. Rev. Rheumatol.* **11**, 606-615.
- Pirola, L., Zvelebil, M. J., Bulgarelli-Leva, G., Van Obberghen, E., Waterfield, M. D. and Wymann, M. P. (2001) Activation loop sequences confer substrate specificity to phosphoinositide 3-kinase alpha (PI3Kalpha). Functions of lipid kinase-deficient PI3Kalpha in signaling. *J. Biol. Chem.* **276**, 21544-21554.
- Rasmussen, A. L., Wang, I. M., Shuhart, M. C., Proll, S. C., He, Y., Cristescu, R., Roberts, C., Carter, V. S., Williams, C. M., Diamond, D. L., Bryan, J. T., Ulrich, R., Korth, M. J., Thomassen, L. V. and Katze, M. G. (2012) Chronic immune activation is a distinguishing feature of liver and PBMC gene signatures from HCV/HIV coinfecting patients and may contribute to hepatic fibrogenesis. *Virology* **430**, 43-52.
- Reddy, V. A. and Rao, N. A. (1976) Dihydrofolate reductase from soybean seedlings. Characterization of the enzyme purified by affinity chromatography. *Arch. Biochem. Biophys.* **174**, 675-683.
- Romas, E., Gillespie, M. T. and Martin, T. J. (2002) Involvement of receptor activator of NFkappaB ligand and tumor necrosis factor-alpha in bone destruction in rheumatoid arthritis. *Bone* **30**, 340-346.
- Rommel, C., Camps, M. and Ji, H. (2007) PI3K delta and PI3K gamma: partners in crime in inflammation in rheumatoid arthritis and beyond? *Nat. Rev. Immunol.* **7**, 191-201.
- Rosengren, S., Corr, M., Firestein, G. S. and Boyle, D. L. (2012) The JAK inhibitor CP-690,550 (tofacitinib) inhibits TNF-induced chemokine expression in fibroblast-like synoviocytes: autocrine role of type I interferon. *Ann. Rheum. Dis.* **71**, 440-447.
- Tabas, I. (2010) Macrophage death and defective inflammation resolution in atherosclerosis. *Nat. Rev. Immunol.* **10**, 36-46.
- Takayanagi, H., Iizuka, H., Juji, T., Nakagawa, T., Yamamoto, A., Miyazaki, T., Koshihara, Y., Oda, H., Nakamura, K. and Tanaka, S. (2000) Involvement of receptor activator of nuclear factor kappaB ligand/osteoclast differentiation factor in osteoclastogenesis from synoviocytes in rheumatoid arthritis. *Arthritis Rheum.* **43**, 259-269.
- Udagawa, N. (2003) The mechanism of osteoclast differentiation from macrophages: possible roles of T lymphocytes in osteoclastogenesis. *J. Bone Miner. Metab.* **21**, 337-343.
- Udalova, I. A., Mantovani, A. and Feldmann, M. (2016) Macrophage heterogeneity in the context of rheumatoid arthritis. *Nat. Rev. Rheumatol.* **12**, 472-485.
- Vanhaesebroeck, B., Leevers, S. J., Panayotou, G. and Waterfield, M. D. (1997) Phosphoinositide 3-kinases: a conserved family of signal transducers. *Trends Biochem. Sci.* **22**, 267-272.
- Vitale, R. F. and Ribeiro Fde, A. (2007) The role of tumor necrosis factor-alpha (TNF-alpha) in bone resorption present in middle ear cholesteatoma. *Braz. J. Otorhinolaryngol.* **73**, 117-121.
- Weitzmann, M. N., Cenci, S., Rifas, L., Brown, C. and Pacifici, R. (2000) Interleukin-7 stimulates osteoclast formation by up-regulating the T-cell production of soluble osteoclastogenic cytokines. *Blood* **96**, 1873-1878.
- Wetzker, R. and Rommel, C. (2004) Phosphoinositide 3-kinases as targets for therapeutic intervention. *Curr. Pharm. Des.* **10**, 1915-1922.
- Wymann, M. P. and Pirola, L. (1998) Structure and function of phosphoinositide 3-kinases. *Biochim. Biophys. Acta* **1436**, 127-150.
- Yokota, K., Sato, K., Miyazaki, T., Kitaura, H., Kayama, H., Miyoshi, F., Araki, Y., Akiyama, Y., Takeda, K. and Mimura, T. (2014) Combination of tumor necrosis factor alpha and interleukin-6 induces mouse osteoclast-like cells with bone resorption activity both *in vitro* and *in vivo*. *Arthritis Rheumatol.* **66**, 121-129.
- Yu, J., Wjasow, C. and Backer, J. M. (1998) Regulation of the p85/p110alpha phosphatidylinositol 3'-kinase. Distinct roles for the n-terminal and c-terminal SH2 domains. *J. Biol. Chem.* **273**, 30199-30203.
- Yu, W., Sun, X., Tang, H., Tao, Y. and Dai, Z. (2010) Inhibition of class II phosphoinositide 3-kinase gamma expression by p185(Bcr-Abl) contributes to impaired chemotaxis and aberrant homing of leukemic cells. *Leuk. Lymphoma* **51**, 1098-1107.
- Zheng, Y., Sun, L., Jiang, T., Zhang, D., He, D. and Nie, H. (2014) TNF alpha promotes Th17 cell differentiation through IL-6 and IL-1beta produced by monocytes in rheumatoid arthritis. *J. Immunol. Res.* **2014**, 385352.